Biogeosciences Discuss., 10, 4819–4850, 2013
www.biogeosciences-discuss.net/10/4819/2013/
doi:10.5194/bgd-10-4819-2013
© Author(s) 2013. CC Attribution 3.0 License.

Biogeosciences Discussions
Open Access

This discussion paper is/has been under review for the journal Biogeosciences (BG).
Please refer to the corresponding final paper in BG if available.

Spatiotemporal distributions of Fukushima-derived radionuclides in surface sediments in the waters off Miyagi, Fukushima, and Ibaraki Prefectures, Japan

M. Kusakabe, S. Oikawa, H. Takata, and J. Misonoo

Marine Ecology Research Institute, Tohwa-Edogawbashi Bldg., 347 Yamabuki-cho, Shinjuku-ku, Tokyo, 162-0801, Japan

Received: 28 December 2012 – Accepted: 13 January 2013 – Published: 11 March 2013

Correspondence to: M. Kusakabe (kusakabe@kaiseiken.or.jp)

Published by Copernicus Publications on behalf of the European Geosciences Union.

Abstract

Spatiotemporal distributions of anthropogenic radionuclides in surface sediments off Miyagi, Fukushima, and Ibaraki Prefectures were analyzed on the basis of data collected during the monitoring program launched by the Japanese Ministry of Education, Sports, Science and Technology in 2011 right after the Fukushima Nuclear Power Plant accident. Concentrations of ^{137}Cs in the surface sediments varied spatially by two orders of magnitude from 1.7 to 580 Bq kg-dry^{-1}, and there was no obvious correlation between ^{137}Cs concentration and the proximity of the sampling location to the site of the accident. The total inventory of ^{137}Cs accumulated in the upper 3 cm of surface sediment in the monitoring area was estimated to be 3.78×10^{13} Bq, that is 0.1–2 % of the total ^{137}Cs flux from the plant to the ocean as a result of the accident (the percentage depends on the model used to estimate the total flux). The spatial variations of ^{137}Cs concentration and inventory depended on two main factors: the ^{137}Cs concentration in the overlying water during the first several months after the accident and the physical characteristics of the sediment (water content and bulk density). The temporal variations of the concentrations of other anthropogenic radionuclides (^{90}Sr, ^{95}Nb, ^{110m}Ag, ^{125}Sb, ^{129}Te, and ^{129m}Te) in the sediments were also investigated. The temporal variations of the activity ratios of these nuclides to ^{137}Cs suggest that before the Fukushima-derived nuclides became homogeneous in seawater, they were removed from the water to the sediment.

1 Introduction

Since 1983, the Marine Ecology Research Institute has been monitoring radioactivity in seawater, sediments, and marine life (e.g. fish, squid) in the coastal areas near nuclear power plants all over Japan under contract with the Japanese Ministry of Education, Sports, Science and Technology (MEXT). During the monitoring period, ^{137}Cs concentrations in the surface sediments collected from coastal waters off the Fukushima

BGD
10, 4819–4850, 2013

Daiichi Nuclear Power Plant (FDNPP) and the neighboring Fukushima Dai-ni Nuclear Power Plant have been declining with time owing to radioactive decay and other mechanisms including vertical mixing of sediments by benthic animals and lateral migration of resuspended sediments (Fig. 1).

Damage to the FDNPP caused by the Great East Japan Earthquake and subsequent tsunami on 11 March 2011 resulted in the release of large amounts of radionuclides to the surrounding environment. Radionuclides were introduced into the ocean both directly, by the release of contaminated water from the power plant, and indirectly, through atmospheric deposition. Fluvial transport of radionuclides from the land to the ocean may be additional pathway. Immediately after the accident, MEXT launched an intensified monitoring program to investigate the impact of the accident on the waters off Fukushima Prefecture, and the contiguous prefectures Miyagi and Ibaraki.

On the basis of the monitoring data and additional complementary data, we report the distributions and inventories of anthropogenic radionuclides derived from the FDNPP in surface sediments collected from May 2011 to February 2012, and we discuss the mechanism by which the radionuclides were deposited on the sediments.

2 Materials and methods

2.1 Collection of sediment samples

From May to July 2011, bottom sediment samples were collected on six sampling dates at each of 12 stations (Fig. 2). From September 2011 to February 2012 sediments were collected on four sampling dates from an expanded monitoring area that included the original 12 stations and 18 additional stations (Fig. 2). See Supplement Table S1 for detailed information about the sampling dates and locations. The sediment samples were retrieved with a multiple corer equipped with eight plastic tubes (opening diameter, 8.2 cm), and the upper 3 cm of the eight sediment cores were combined. Approximately 2 kg of each combined wet sediment sample was refrigerated immediately on board the

BGD
10, 4819–4850, 2013

sampling vessel and saved for analysis. In many cases, two or more sampling casts were necessary to obtain 2 kg samples. The wet sediment samples packed in a 120 ml plastic bottle were used for measurement of the bulk density and water content of the sediments by gravimetric method in a laboratory on land. The remainder of each sample was dried at 105 °C, ground in a mortar, sieved through a screen (mesh size, < 2 mm), mixed well, and then pulverized to a homogeneous powder in a table top grinder.

2.2 Determination of ^{134}Cs, ^{137}Cs, ^{131}I, and other gamma-ray-emitting nuclides

An aliquot of each dried sediment sample (400–600 g) was placed in a plastic container and analyzed by means of nondestructive gamma-ray spectrometry with a Ge detector. The detection limits for ^{134}Cs, ^{137}Cs and ^{131}I (calculated as three times the fluctuation inherent in the background) were approximately 1, 1 and 0.8 Bq kg-dry^{-1}, respectively, over a counting period of tens of thousands of seconds. We also determined ^{95}Nb, ^{110m}Ag, ^{125}Sb, ^{129m}Te and ^{129}Te, and the detection limits for these radionuclides were almost the same as or lower than those of ^{134}Cs and ^{137}Cs, depending on the branching ratio and the gamma-ray energy

2.3 Determination of ^{90}Sr and ^{89}Sr

Owing to the time-consuming chemical procedure required for measurement, ^{90}Sr concentrations in the sediments were measured only in samples containing relatively high concentrations of ^{137}Cs.

Strontium was extracted from 300 g aliquots of dried bottom sediment with 7 M nitric acid after the addition of a known amount of a stable Sr^{2+} carrier. Strontium was precipitated from the supernatant as strontium oxalate, which was collected by filtration and incinerated at 600 °C for 3 h. The incineration residue was dissolved in a few volumes of concentrated nitric acid, and the Sr in the resulting nitric acid solution was purified by successive co-precipitation with ferric hydroxides and barium chromate ($BaCrO_4$).

BGD
10, 4819–4850, 2013

The decay product of ^{90}Sr, ^{90}Y was removed by co-precipitation with ferric hydroxides, and then the supernatant solution was allowed to stand for approximately 2 weeks. The ^{90}Sr concentrations were determined by measuring the beta-rays emitted from ^{90}Y in radioactive equilibrium with ^{90}Sr by means of a gas-flow-type low-background anticoincidence beta counter (LBC-471Q, Aloka Co. Japan). The detection limits, which were calculated as three times the background fluctuation, depended on counting time and sample volume and were approximately 0.8 Bq kg-dry^{-1} from May to July 2011 and 0.3 Bq kg-dry^{-1} from September 2011 to February 2012.

The analytical procedure was modified as follows for the samples that were used to measure both ^{89}Sr and ^{90}Sr. After the dried samples were dissolved in concentrated nitric acid with an added Sr^{2+} carrier, Sr was purified with an anion-exchange resin and then precipitated as $SrCO_3$. Beta-rays emitted from the $SrCO_3$ by the decay of ^{89}Sr, ^{90}Sr and ^{90}Y were measured. The ^{90}Y was milked from the $SrCO_3$ and its beta-ray emissions were measured to evaluate ^{90}Sr activity (MEXT 2002). The detection limit for ^{89}Sr was estimated to be 0.8 Bq kg-dry^{-1}.

3 Results and discussion

Most of the data used in this study are available on the MEXT website (http://radioactivity.mext.go.jp/en/list/259/list-1.html). Data obtained during the course of the monitoring project that are relevant to the current study are also provided in Supplement Tables S1–S3.

3.1 Distribution of ^{137}Cs in the sediments

The ^{137}Cs concentrations in the surface sediments varied tremendously with respect to both time and space (Fig. 3), ranging from 1.7 to 580 Bq kg-dry^{-1} over the course of the entire sampling period (May 2011 to February 2012). The concentrations were at most two orders of magnitude greater than the concentrations measured in 2010 at

BGD
10, 4819–4850, 2013

eight sampling stations off Fukushima Prefecture (MEXT 2011; Fig. 1). Although the stations in the northernmost and southernmost parts of the monitoring area (e.g. A1, A3, L1, and L3) were influenced the least by the accident, close proximity of a sampling station to the FDNPP did not necessarily result in a high ^{137}Cs concentration. From May to July 2011 when sampling was restricted to areas relatively close to the coast, the concentrations were higher at the northern stations (e.g. B1, C1, and D1) than the rest of the stations, and the concentration was also consistently high at Stn. J1. From September 2011 to February 2012, the concentration at Stn. B3 was substantially higher than at the other stations. Note that monitoring at Stn. B3 was not conducted prior to September 2011.

The temporal variations of the ^{137}Cs concentrations at all the stations are shown in Fig. 4. Early in the sampling period (May-June 2011), the concentrations varied considerably with sampling date especially for the stations in the southern portion of the monitoring area (e.g. I1, J1, K1, and L1). After September 2011, however, there was generally much less temporal variation of the concentrations. There are several possible explanations for the observed variability of the ^{137}Cs concentrations in the sediments throughout the monitoring period.

One explanation is mobility of the topmost layer of sediment. Because the surface sediment layer enriched with ^{137}Cs is supposed to be thin due to its short accumulation period from March 2011 to February 2012, it can be remobilized by bottom-water turbulence, especially in coastal waters. Otosaka and Kobayashi (2012) suggested that radiocesium is transported laterally by resuspended sediments. If this is the case, then the physics of the bottom water can be expected to play an important role in the variability of ^{137}Cs concentration.

Another possible explanation is local heterogeneity in the physical and chemical characteristics of the sediments, which affect incorporation of Cs from seawater into the sediments. For evaluation of the effects of sediment heterogeneity, six bottom sediment samples were collected in succession at Stn. D1 on 13 September 2011, and their ^{137}Cs concentrations and ^{134}Cs/^{137}Cs activity ratios were determined (Fig. 5).

BGD
10, 4819–4850, 2013

Although the activity ratios were relatively constant, meaning that the isotopes had a common origin, the ^{137}Cs concentrations ranged from 17 to 580 Bq kg-dry^{-1}, with an average and standard deviation of 330 ± 160 Bq kg-dry^{-1} Thus, some of the variation of the concentrations shown in Figs 3 and 4 likely reflected local heterogeneity of the ^{137}Cs concentrations in the sediments

Another possible explanation is sampling artifacts resulting from loss of surface sediment during sample retrieval. However, this explanation is unlikely because the multiple corer used to collect the samples usually preserves surface sediment intact. In addition, although we used a global positioning system to locate the predefined sampling stations, positional deviations due to current and wind were inevitable, as indicated by the fact that there was a great deal of scatter in data from a given station in different years (Fig. 1).

Finally, the pathways for nuclide migration to the sediments may have been variable, and this possibility is discussed in Sect. 3.4.

3.2 Distribution of ^{134}Cs in the sediments

The distribution of FDNPP-derived ^{134}Cs, which has a shorter half-life (2.06 yr) than ^{137}Cs, is expected to be identical to that of ^{137}Cs except for differences due to decay. We plotted the temporal variation of the ^{134}Cs/^{137}Cs ratio in the sediments (Fig. 6), and a weighted least-squares fit of the data indicated that the ratio decreased with time at a first-order rate of -8.68×10^{-4} day^{-1}, which is equivalent to a half-life of 2.18 yr and thus agrees well with the known half-life of ^{134}Cs. The good corelation ($R^2 = 0.73$) of the fit indicates that the ^{134}Cs distribution mimicked that of ^{137}Cs. The fit equation gave an intercept of 0.989 on 11 March 2011, which agrees well with the ratio for seawater (0.93) reported by Oikawa et al. (2013) and other investigators (e.g. Buesseler et al., 2012; Aoyama et al., 2012).

BGD
10, 4819–4850, 2013

3.3 Inventory of ^{137}Cs in the sediments

Inventories of ^{137}Cs (I_{Cs}, Bq m^{-2}) in the upper 3 cm of sediment were calculated from sediment bulk densities (D_s), water contents (W_s), and ^{137}Cs concentrations (C_{Cs}, Bq kg-dry^{-1}):

$$I_{Cs} = D_s(1 - W_s)C_{Cs} \times 3 \times 1000$$

and the results are plotted in Fig. 7. The spatial distribution patterns of the inventories were generally similar to the concentration patterns, with some notable exceptions. For example, although the concentrations at Stn. B3 were consistently high (Fig. 2), the inventory at that station was not particular high compared to the inventories at the other stations. ^{137}Cs concentrations and inventories were linearly correlated (Fig. 8), but the slope varied with bulk density.

On the basis of the estimated area (22 177 km^2, Fig. 2) and the average inventory (0.161 Bq cm^{-2}) for the last sampling date (February 2012), we calculated the total amount of ^{137}Cs in the monitoring area to be 3.78×10^{13} Bq. This value is clearly an underestimate of the actual value because the inventory data were restricted to the upper 3 cm of sediment and the monitoring area did not cover the entire contaminated area. Otosaka and Kobayashi (2012) detected Fukushima-derived ^{137}Cs below the upper 3 cm of sediment, and ^{137}Cs penetrated deeper into sandy sediment than into clay sediment.

Various estimates of the total amount of ^{137}Cs directly released to the ocean following the accident at FDNPP have been reported, ranging from 2×10^{15} to 15×10^{16} Bq depending on the model used (Masumoto et al., 2012). In addition, Bailly du Bois et al. (2012) recently calculated the amount to be 27×10^{16} Bq. The contribution of airborne ^{137}Cs to the ocean inventory may not be significant. The amount of ^{137}Cs discharged into the atmosphere was estimated to be 1.3×10^{16} Bq (Chino et al., 2011), and the amount deposited from the atmosphere to the ocean over an 80-km radius from the FDNPP was estimated to be 76×10^{13} Bq (Bailly du Bois et al., 2012) If we use our

BGD
10, 4819–4850, 2013

estimated value of 3.78×10^{13} Bq as the total inventory of ^{137}Cs in the monitoring area as of February 2012, 0.1–2 % of the total ^{137}Cs flux from the plant to the ocean was deposited onto the bottom sediment, with the percentage depending on which estimate of the total ^{137}Cs flux was used. More accurate quantification of the mass balance of ^{137}Cs in the coastal ocean will require expansion of the monitoring area especially in proximity to the FDNPP, detailed study of the vertical profile of ^{137}Cs in the sediment and a more accurate evaluation of its flux to the ocean.

Because it is important to determine whether the total inventory of ^{137}Cs in sediment was increased as a result of the accident at Fukushima we roughly estimated the temporal variation of ^{137}Cs inventories. Average inventories were determined for sediments samples collected over the entire 10-month sampling period (Table 1) at stations with designations including the number 1 (A1, B1, etc.) and for sediment samples collected over the 6-month period starting in September 2011 at all the stations. The average inventories for the former set of stations were highly variable and did not show any clear increasing trend; whereas the inventories appeared to decrease from September 2011 onward (Table 1), as did the inventories for all the sediment samples collected in the monitoring area (enclosed by the red dashed line in Fig. 2). Specifically, the total inventory of ^{137}Cs in the monitoring area decreased from 5.16×10^{13} Bq in September 2011 to 3.78×10^{13} Bq in February 2012 (Table 1). However, because of the above-mentioned variability of the ^{137}Cs concentration in the samples collected repeatedly from the same station (Fig. 5), concluding that the inventory showed a decreasing trend would be premature. If the total inventory of ^{137}Cs in the upper 3 cm of sediment did in fact decrease, the decrease might have been due to bioturbation that carried Cs deeper into the sediment or to lateral transport of resuspended sediment to the open ocean as suggested by Otosaka and Kobayashi (2012).

BGD
10, 4819–4850, 2013

3.4 Removal of ^{137}Cs from seawater to the sediment

The concentration of ^{137}Cs in the sediment samples depended on the type of sediment. Sediment bulk density and ^{137}Cs concentration were inversely correlated; that is, sediments with higher bulk densities had lower Cs concentrations (Fig. 9). Results from monitoring in the same area prior to the FDNPP accident suggest that sediment with relatively low bulk density has a finer grain size (i.e. clay) and abundant organic matter content (Marine Ecology Research Institute, unpublished data). These results imply that Cs tended to concentrate preferentially on sediments that were fine grained, rich in organic matter, or both. The strong affinity of Cs for clay minerals is well documented (e.g. Børrentzen and Salbu, 2002; Tsukada, et al., 2008; Qin et al., 2012). Otosaka and Kobayashi (2012) measured Fukushima-derived ^{137}Cs concentrations in coastal sediments off Ibaraki Prefecture and showed that fine-grained sediments have higher ^{137}Cs concentrations than coarse-grained sediments. However, the scatter of the data in Fig. 9 indicates that sediment mineralogy alone cannot completely account for the spatial distribution of ^{137}Cs in the sediments.

The concentration of ^{137}Cs in the surface water above the sediment can be expected to affect the concentrations in the sediment. The rate of ^{137}Cs release to the ocean reached its maximum value ($\sim 0.1\,\mathrm{PBq\,day^{-1}}$) in early April and then began to decrease exponentially (Kawamura et al., 2011; Tsumune et al., 2012). On 14 April, the ^{137}Cs concentration in the surface water reached its maximum of $\sim 190\,\mathrm{Bq\,L^{-1}}$ at Stn. 4 (~ 4 km away from Stn. E1), where a sediment sample swas not collected (Oikawa et al., 2013). After that date, the concentration in the surface water decreased exponentially. In July, the maximum concentration was $\sim 1\,\mathrm{Bq\,L^{-1}}$. From April to July, the ^{137}Cs inventory in a 100×50 km box off Fukushima declined by almost four orders of magnitude (Bailly du Bois et al., 2012). Thus, the majority of ^{137}Cs released from the FDNPP can be accounted for by integration of ^{137}Cs concentrations in the surface water from April to July.

BGD
10, 4819–4850, 2013

We investigated the relationship between ^{137}Cs concentrations integrated from May to July 2011 in the surface seawater (< 5 m depth) and concentrations in sediments averaged from September 2011 to February 2012 (Fig. 10). The average concentration of ^{137}Cs in surface sediment was positively correlated with the integrated seawater concentration at each station, but in sediments with relatively high bulk density (that is, sandy sediments), the ^{137}Cs concentrations were lower (Stns. L1, K1, I3, B1, and C1). The data in the figure suggest that almost all the ^{137}Cs in the sediment had accumulated by the end of July 2011 and that the higher ^{137}Cs concentrations in sediment were derived from higher concentrations in the overlying surface seawater. ^{137}Cs is associated with sediments that have relatively low bulk density and that are rich in clay organic matter, or both. In other words, fine settling particles enriched in ^{137}Cs accumulated in areas where they could reach the bottom without being disturbed by strong turbulence. Oikawa et al. (2013) qualitatively described a scenario for the migration of surface ^{137}Cs after the accident as follows: in early May all the ^{137}Cs-polluted water migrated north and in the end of May some of it went south to around Stns. I1, J1, and K1 while the remainder stayed at around Stn. B1 and B3. Two water masses with high ^{137}Cs concentrations in the south and north persisted at least until July. These investigators' interpretation of the surface distribution is in accordance with the sediment distribution: that is, relatively high concentrations in the north (e.g. at Stn. B3) and in the south (e.g. at Stn. J1). Admittedly the scenario presented here is crude because of the lack of seawater concentration data in April 2011. Simulation results reported by Tsumune et al. (2012), however, suggest that the influence of highly polluted water was restricted to a relatively small portion of the monitoring area so that the overall trend shown in Fig. 10 may not be affected by the lack of the data in April 2011.

This scenario is based on the assumption that Cs removal from seawater occurs rapidly enough that the distribution of Cs in the sediment reflects that of the directly overlying seawater. Cesium is soluble in seawater, but once it is incorporated into particles, it is rapidly removed from seawater to the bottom sediment. Fowler et al. (1987) observed that Chernobyl-derived radionuclides including ^{137}Cs were transported from

BGD
10, 4819–4850, 2013

the surface of the Black Sea to a depth of 200 m in a few days. These investigators emphasized the importance of large, dense fecal pellets of zooplankton as nuclide carriers. Kusakabe et al. (1988) estimated the settling velocities of Chernobyl-derived particulate ^{137}Cs to be 60–190 m day^{-1} in the northern North Pacific. Fast removal of particulate Cs may result in a relatively good relationship between the integrated concentration of ^{137}Cs in surface seawater and the average ^{137}Cs concentration in sediment. The possibility of fast removal of nuclides from seawater is also described in Sects. 3.5 and 3.7.

3.5 Distribution of ^{131}I in the sediments

The concentration of ^{131}I in the sediments reached a maximum of 6.1 Bq kg-dry^{-1} at Stn. G1 on 9 May 2011 and then decreased quickly owing to its short half-life of 8 days (Fig. 11). ^{131}I was last detected on 8 June 2011 (1.3 Bq kg-dry^{-1} at Stn. J1) and since then no ^{131}I has been detected in the sediments.

During the monitoring program off Fukushima, seawater and airborne dust were analyzed for radioactivity (MEXT 2012), and we compared the ^{131}I/^{137}Cs activity ratios in sediments with the ratios in airborne dust and seawater (Fig. 11). The concentration of ^{131}I in dust, which was measured from 23 March in the waters in the vicinity of the FDNPP, reached a maximum at the end of March, and decreased to below the detection limit by 7 April (MEXT 2011). The ^{131}I/^{137}Cs activity ratios in dust and seawater varied by an order of magnitude in the middle of April, and the ratios in seawater seems to converged to a value that followed its decay trend since then. On the basis of an analysis of ^{131}I/^{137}Cs activity ratios in seawater 30 km off the FDNPP, Tsumune et al. (2012) inferred that although both nuclides in the area were derived mainly from the atmosphere until 9 April 2011, they were dominated by direct discharge after that date. The ^{131}I/^{137}Cs ratio at the discharge site on 26 March 2011 was estimated to be 5.7. The theoretical decay curve based on this estimate (see the line in Fig. 11) indicates that although the ratios in the sediments fell along the line, the scatter about the line was greater for the sediments than seawater in April. Several points of deviation from

BGD
10, 4819–4850, 2013

the line may have been due to atmospheric input, the ratios of which vary with time (Chino et al., 2011).

The chemistries of I and Cs in seawater are different especially in terms of their removal from seawater. For example, the distribution coefficients, K_d, of I and Cs in the marginal sea are 7×10^1 and 4×10^3, respectively (IAEA, 2004), the indication being that Cs is more easily adsorbed onto or incorporated into particles than I, and as a result the $^{131}I/^{137}Cs$ ratios in sediments should be smaller than those in seawater. However, the data in Fig. 11 do not show such a consistent trend and may reflect the variability of the $^{131}I/^{137}Cs$ ratios in seawater and dust, implying that both nuclides were removed from seawater to the sediment at the same time in a short period of time.

3.6 Distribution of ^{90}Sr in the sediments

Five sediment samples were analyzed for ^{89}Sr (Supplement Table S3), but none of them had a ^{89}Sr concentration above the detection limit. Concentration of ^{90}Sr in surface seawater was measured from August to November 2011, showing only 2–4 fold increase compared to pre-accident values, unlike ^{137}Cs, which showed about 2 orders of magnitudes increase in the same period (Oikawa et al., 2013). ^{90}Sr was not detected in the sediments collected from May to July 2011 probably owing to the relatively high detection limit (see Sect. 2.3). The concentrations in the samples collected starting in September 2011 ranged from 0.1 to 1.9 Bq kg-dry^{-1}, but most of the data fell in the range from 0.1 to 0.3 Bq kg-dry^{-1} (Fig. 12). Note that the data below the detection limit are not plotted in the figure. A much higher concentration (1.9 Bq kg-dry^{-1}) was measured at Stn. J1. Unfortunately, background ^{90}Sr concentrations in the area before the accident are not available. However, ^{90}Sr has been measured in the sediments collected from the waters off Aomori and Iwate Prefectures which are next to Miyagi Prefecture; the measured concentrations range from 0 (below the detection limit) to 0.51 Bq kg-dry^{-1} (MEXT, 2011). Thus, the ^{90}Sr concentrations that we measured seem to indicate that the sediments were not contaminated by Fukushima-derived Sr. The high ^{90}Sr concentration in the sediment collected from Stn. J1 may not have been due

BGD
10, 4819–4850, 2013

to the accident, because ^{89}Sr, which has a half-life of 50.5 days and is believed to be a Fukushima-derived radioisotope, was not detected. The reason for the high ^{90}Sr concentration at Stn. J1 is unknown.

Most of the ^{90}Sr/^{137}Cs activity ratios were below 0.001 (Fig. 12). In 2010, the average ^{90}Sr/^{137}Cs ratio in surface sediments off Aomori Prefecture (to the north of Fukushima) was 0.11 and that in seawater was 0.79 (MEXT, 2011). Although these sampling areas off Aomori and Fukushima do not overlap each other, the lack of a significant change in the ^{90}Sr concentration and the lower ^{90}Sr/^{137}Cs activity ratio after the accident can be explained only by preferential removal of Cs over Sr. The fact that the K_d value of Sr for the marginal sea was estimated to be 8, three orders of magnitude smaller than the K_d of Cs (4×10^3), supports the idea that Cs was preferentially removed (IAEA, 2004).

3.7 Distributions of other radionuclides in the sediments

We also detected the following nuclides in the sediments: ^{95}Nb ($t_{1/2}$ = 35 days), ^{110m}Ag ($t_{1/2}$ = 250 days), ^{129}Te ($t_{1/2}$ = 69.6 min), ^{129m}Te ($t_{1/2}$ = 33.6 days), and ^{125}Sb ($t_{1/2}$ = 2.8 y). Their concentrations and activity ratios with respect to ^{137}Cs are plotted in Fig. 13 Because ^{129m}Te ($t_{1/2}$ = 33.6 days) has a shorter-lived progeny nuclide, ^{129}Te ($t_{1/2}$ = 69.6 min), the two nuclides should have been in radioactive equilibrium in the sediment. We calculated an average ^{129m}Te/^{129}Te activity ratio of 0.68 ± 0.14, which agrees well with the isomeric transition rate of ^{129m}Te relative to that of ^{129}Te, 0.647. Accordingly the variation patterns of the two nuclides were almost identical to each other.

The concentrations of the nuclides plotted in Fig. 13 varied significantly among the sampling stations. In addition the temporal variation of the activity ratios relative to ^{137}Cs, especially those of ^{95}Nb and ^{110m}Ag, did not necessarily agree with the theoretical decay curves indicated by the blue lines in Fig. 13. Furthermore, when the ratios were decay-corrected to 11 March 2011, the calculated ratios were scattered over an order of magnitude range. Variable activity ratios for Fukushima-derived radionuclides

BGD
10, 4819–4850, 2013

in soil have been reported (e.g. Watanabe et al., 2012; Yoshida et al., 2012). These investigators ascribed the variability to the variable initial ratios at the accident site.

The activity ratios of ^{95}Nb, ^{110m}Ag, ^{129}Te, ^{129m}Te, and ^{125}Sb to ^{137}Cs calculated for the samples from Stn. D1 collected on 13 September 2011 also varied greatly. The complexity of their spatiotemporal variations in the sediments may have been due to temporal changes of the activity ratios from the FDNPP and the fluctuating pathways by which these nuclides reached the sediments. As mentioned above for ^{131}I, this hypothesis is valid only if the nuclides stayed in the seawater for a short time.

4 Conclusions

The distributions of anthropogenic radionuclides in surface sediments collected from the waters off Fukushima Prefecture were complicated reflecting variability in the characteristics of the bottom sediment and variability in the nuclide concentrations in the overlying water. Rapid removal of the nuclides, except for ^{90}Sr, from seawater to the sediment also contributed to the variations in their distributions. The mechanism by which the radionuclides were incorporated into the sediment has yet to be elucidated fully. Biological activity may have played an important role, and the unusual sedimentary environment resulting from the huge suspended load carried back from the land by the tsunami may have led to rapid removal of the nuclides from seawater.

The fate of the nuclides in sediments is of great concern to the people of Japan and to the global community. Because nuclide concentrations in seawater have been decreasing, deposition from seawater may no longer be significant, unless there are additional releases from the nuclear plant or increased riverine inputs derived from decontamination on land. However, even though the inventories of radionuclides in the sediments seem to be slightly decreasing, the remaining nuclides will not disappear quickly. Continuous, thorough monitoring and detailed research on the behavior of the radionuclides in sediment for many years to come are required.

BGD
10, 4819–4850, 2013

Supplementary material related to this article is available online at: http://www.biogeosciences-discuss.net/10/4819/2013/bgd-10-4819-2013-supplement.zip.

Acknowledgement. We sincerely thank our colleagues at the Marine Ecology Research Institute for their help with sampling and for logistical support for the monitoring program. The crews of the research vessels and technicians from Nippon Kaiyo Co. assisted greatly with fieldwork onboard the ships. This research was conducted under contract with MEXT.

References

Aoyama, M., Tsumune, D., Uematsu, M., Kondo, F., and Hamajima, Y.: Temporal variation of ^{134}Cs and ^{137}Cs activities in surface water at stations along the coastline near the Fukushima Dai-ichi Nuclear Power Plant accident site, Japan. Geochem. J., 46, 321–325, 2012.

Bailly du Bois, P., Laguionie, P., Boust, D., Korsakissok, I., Didier, D., and Fievet, B.: Estimation of marine source-term following Fukushima Dai-ichi accident, J. Environ. Radioactiv., 114, 2–9, 2012.

Børrentzen, P. and Salbu, B.: Fixation of Cs to marine sediments estimated by a stochastic modeling approach, J. Environ. Radioact., 61, 1–20, 2002.

Buesseler, K. O., Jayne, S. R., Fisher, N. S., Rypina, I. I., Baumann, H., Baumann, Z., Breier, C. F., Douglass, E. M., George, J. Macdonald, A. M., Miyamoto, H., Nishikawa, J., Pike, S. M., and Yoshida, S.: Fukushima-derived radionuclides in the ocean and biota off Japan, Proc. Natl. Acad. Sci. USA, 109, 5984–5988, 2012.

Chino, M., Nakayama, H., Nagai, H., Terada, H., Katata, G., and Yamazawa, H.: Preliminary estimation of release amounts of ^{131}I and ^{137}Cs accidentally discharged from the Fukushima Daiichi Nuclear Power Plant into the atmosphere, J. Nucl. Sci. Technol., 48, 1129–1134, 2011.

Fowler, S. W., Buat-Menard, P., Yokoyama, Y., Ballestra, S. Holm, E., and Nguyen, H. V.: Rapid removal of Chernobyl fallout from Mediterranean surface waters by biological activity, Nature, 329, 56–58, 1987.

BGD
10, 4819–4850, 2013

IAEA: Sediment distribution coefficients and concentration factors for biota in the marine environment, Tech. Rep. Ser. no. 422, 2004.
Kawamura, H., Kobayashi, T., Furuno, A., In, T., Ishikawa, Y., Nakayama, T., Shima, S., and Awaji, T.: Preliminary numerical experiments on oceanic dispersion of ^{131}I and ^{137}Cs discharged into the ocean because of the Fukushima Daiichi Nuclear Power Plant Disaster, J. Nucl. Sci. Technol., 48, 1349–1356, 2011.
Kusakabe, M., Ku, T. L., Harada, K., Taguchi, K., and Tsunogai, S.: Chernobyl radioactivity found in mid-water sediment trap interceptor in the N. Pacific and Bering Sea, Geophys. Res. Lett., 15, 44–47, 1988.
Masumoto, Y., Miyazawa, Y., Tsumune, D., Tsubono, T., Kobayashi, T., Kawamura, H., Estournel, C., Marsaleix, P., Lanerolle, L., Mehra, A., and Garraffo, Z. D.: ^{137}Cs released from the Fukushima Daiichi Nuclear Power Plant, Elements, 8, 207–212, 2012.
MEXT: Radioactivity Measurement: Series No. 2, in Japanese, available at: http://www.kankyohoshano.go.jp/series/lib/No2.pdf last access: 24 January 2013, 2002.
MEXT: Report of Comprehensive Monitoring Program for radioactivity in the Marine Environments, 2010, 2011, in Japanese.
MEXT: Report of Comprehensive Monitoring Program for radioactivity in the Marine Environments, 2011, 2012, in Japanese.
Oikawa, S., Takata, H., Watabe, T., Misonoo, J. and Kusakabe, M.: Distribution of the Fukushima-derived radionuclides in seawater in the Pacific off the coast of Miyagi, Fukushima, and Ibaraki Prefectures, Japan, Biogeosciences Discuss., 10, 4851–4886, doi:10.5194/bgd-10-4851-2013, 2013.
Otosaka, S. and Kobayashi, T.: Sedimentation and remobilization of radiocesium in the coastal area of Ibaraki, 70 km south of the Fukushima Dai-ichi Nuclear Power Plant, Environ. Monit. Assess, doi:10.1007/s10661-012-2956-7, 2012.
Qin, H., Yokoyama, Y., Fan, Q., Iwatani, H., Tanaka, K., Sakaguchi, A., Kanai, Y., Zhu, J., Onda, Y., and Takahashi, Y.: Investigation of cesium adsorption on soil and sediment samples from Fukushima Prefecture by sequential extraction and EXAFS technique, Geochem. J., 46, 297–302, 2012.
Tsukada, H., Takeda, A., Hisamatsu, S., and Inaba, J.: Concentration and specific activity of fallout ^{137}Cs in extracted and particle-size fractions of cultivated soils, J. Environ. Radioact., 99, 875–881, 2008.

BGD
10, 4819–4850, 2013

Tsumune, D., Tsubono, T., Aoyama, M., and Hirose, K.: Distribution of oceanic ^{137}Cs from the Fukushima Dai-ichi Nuclear Power Plant simulated numerically by a regional ocean model, J. Environ. Radioactiv., 111, 100–108, 2012.

Watanabe T., Tsuchiya, N., Oura, Y., Ebihara, M., Inoue, C., Hirano, N., Yamada, R., Yamasaki, S., Okamoto, A., Nara, F. W., and Nunohara, K. : Distribution of artificial radionuclides (^{110m}Ag, ^{129m}Te, ^{134}Cs, ^{137}Cs) in surface soils from Miyagi Prefecture, northeast Japan, following the 2011 Fukushima Dai-ichi nuclear power plant accident, Geochem. J., 46, 279–285, 2012.

Yoshida, N. and Takahashi, Y.: Land-surface contamination by radionuclides from the Fukushima Daiichi nuclear power plant accident, Elements, 8, 201–206, 2012.

BGD
10, 4819–4850, 2013

Table 1. Inventories of ^{137}Cs in the upper 3 cm of the surface sediments.

Sampling date	Average inventory (1)[a] ($\times 10^3$ Bq m^{-2})	Average inventory (2)[b] ($\times 10^3$ Bq m^{-2})	Inventory[c] ($\times 10^{13}$ Bq)
09–14 May 2011	2.44	–	–
23–27 May 2011	1.80	–	–
06–10 June 2011	2.40	–	–
20–25 June 2011	2.01	–	–
05–09 July 2011	2.38	–	–
25–31 July 2011	2.50	–	–
07–15 September 2011	2.88	2.20	5.16
13–26 October 2011	2.17	1.91	4.49
05–16 December 2011	1.88	1.81	4.24
04–21 February 2012	1.65	1.61	3.78

[a] Average inventory for the sediments collected at Stns. A1, B1, C1, D1, E1, F1, G1, H1, I, J1, K1, and L1.
[b] Average inventory for all the stations monitored since September 2011.
[c] Total inventory in the area enclosed by the red dashed line in Fig. 1.

BGD
10, 4819–4850, 2013

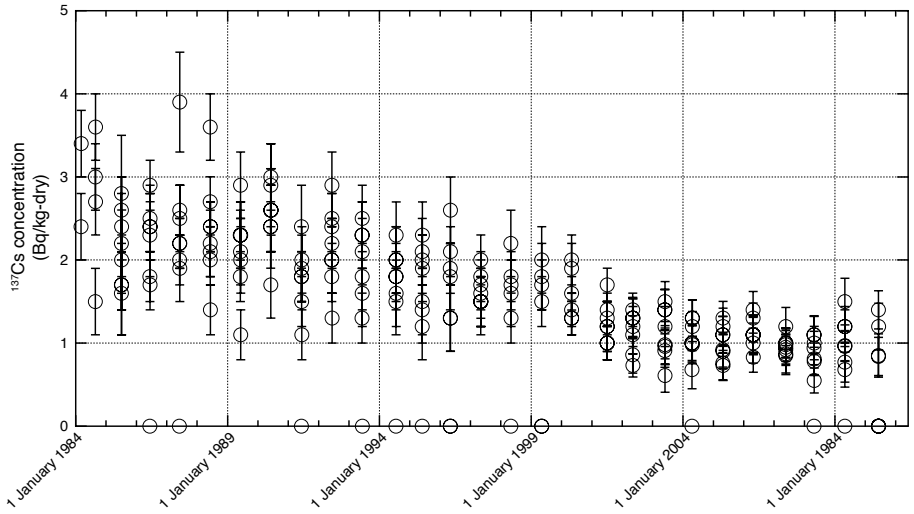

Fig. 1. Temporal variation of ^{137}Cs concentrations in surface sediment collected from the waters off the Fukushima Daiichi and Daini Nuclear Power Plants prior to 2011 (1984–2010). The data plotted in the figure were obtained from MEXT (2011). Eight sampling stations are located about 30 km off the coast. The open circles on the x-axis indicate the concentrations are below the detection limit.

BGD
10, 4819–4850, 2013

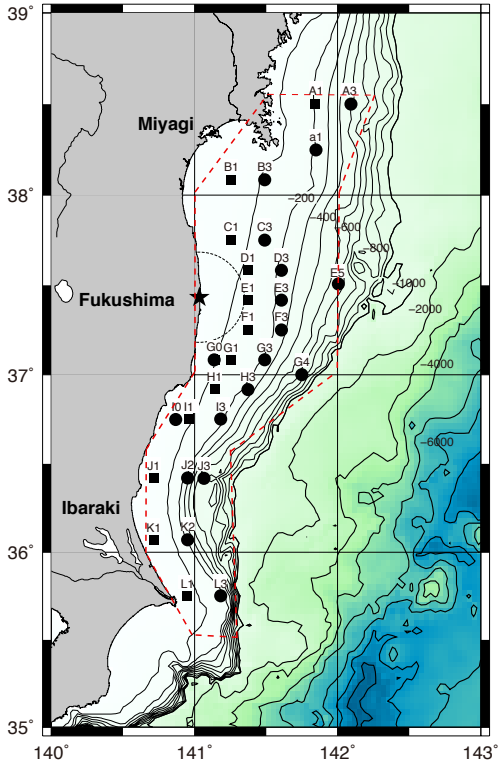

Fig. 2. Locations of sampling stations. Solid squares indicate stations where sediment samples were collected on 10 dates from May 2011 to February 2012 and solid circles indicate stations where samples were collected on 4 dates from September 2011 to February 2012. The star indicates the location of the Fukushima Dai-ichi Nuclear Power Plant, and the dashed black semicircle encloses the area within a 30-km radius of the plant. ^{137}Cs inventories in the sediments were estimated for the area enclosed by the red dashed line (see Sect. 3.1).

BGD
10, 4819–4850, 2013

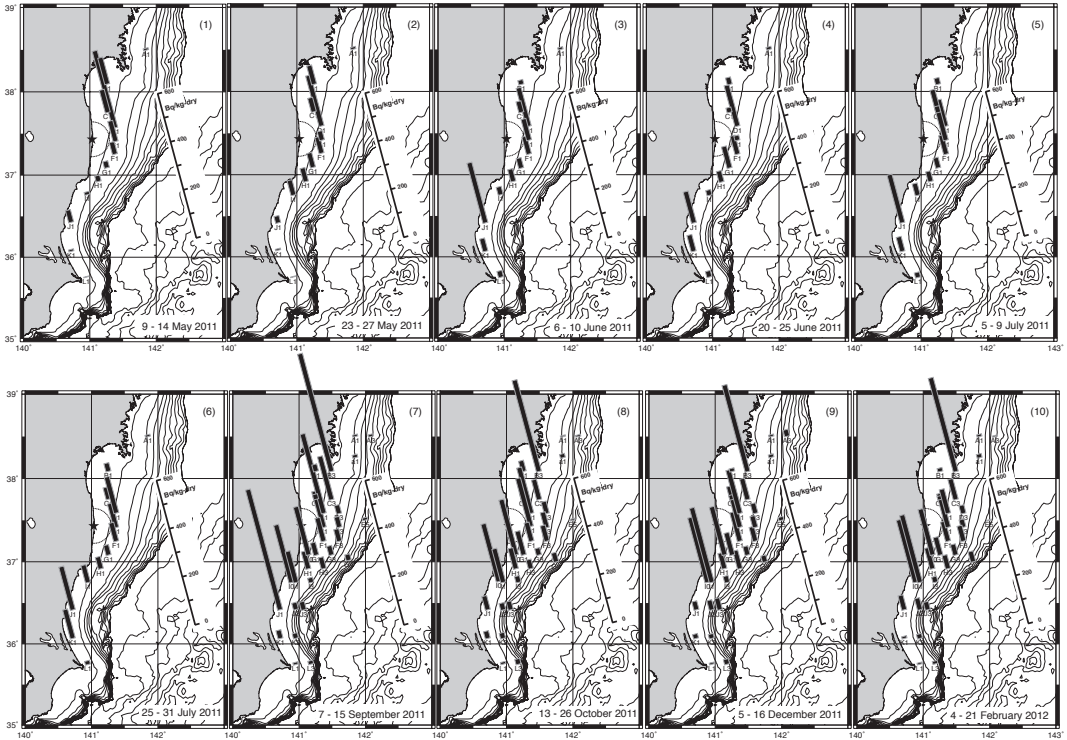

Fig. 3. Spatiotemporal distribution of ^{137}Cs concentrations in sediment samples collected on the dates indicated in the panels. Six sediment samples were collected at Stn. D1 on 13 September 2011, and the average value for the six samples is plotted in the figure (see Sect. 3.1 and Fig. 5).

BGD
10, 4819–4850, 2013

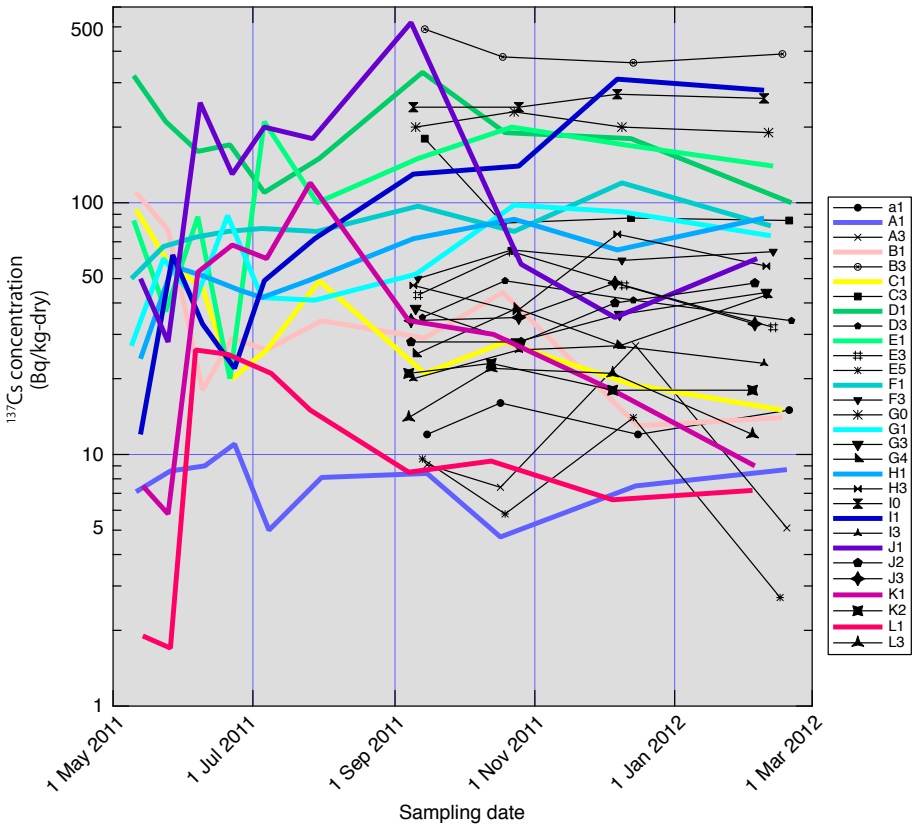

Fig. 4. Temporal variations of ^{137}Cs concentrations in the sediments. Six sediment samples were collected at Stn. D1 on 13 September 2011, and the average of the six concentrations is plotted in the figure (see Sect. 3.1 and Fig. 5).

BGD
10, 4819–4850, 2013

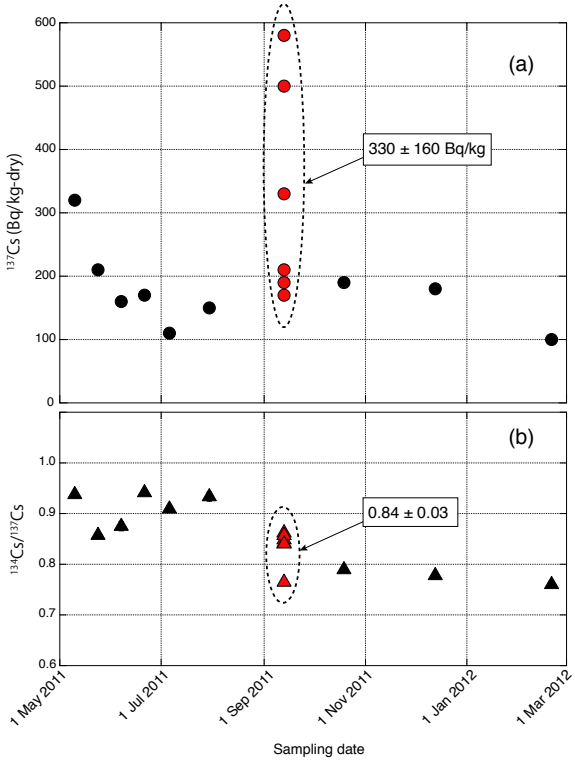

Fig. 5. (a) Temporal variation of ^{137}Cs concentrations in sediment samples collected at Stn. D1 (black circles) and reproducibility as indicated by data for six samples collected on 13 September 2011 (red circles). For each data point, the error is less than or equal to the size of the circle **(b)** Temporal variation of ^{134}Cs/^{137}Cs in sediment samples collected at Stn. D1 (black triangles) and reproducibility as indicated by data for six samples collected on 13 September 2011 (red triangles). For each data point, the error is less than or equal to the size of the triangle.

BGD
10, 4819–4850, 2013

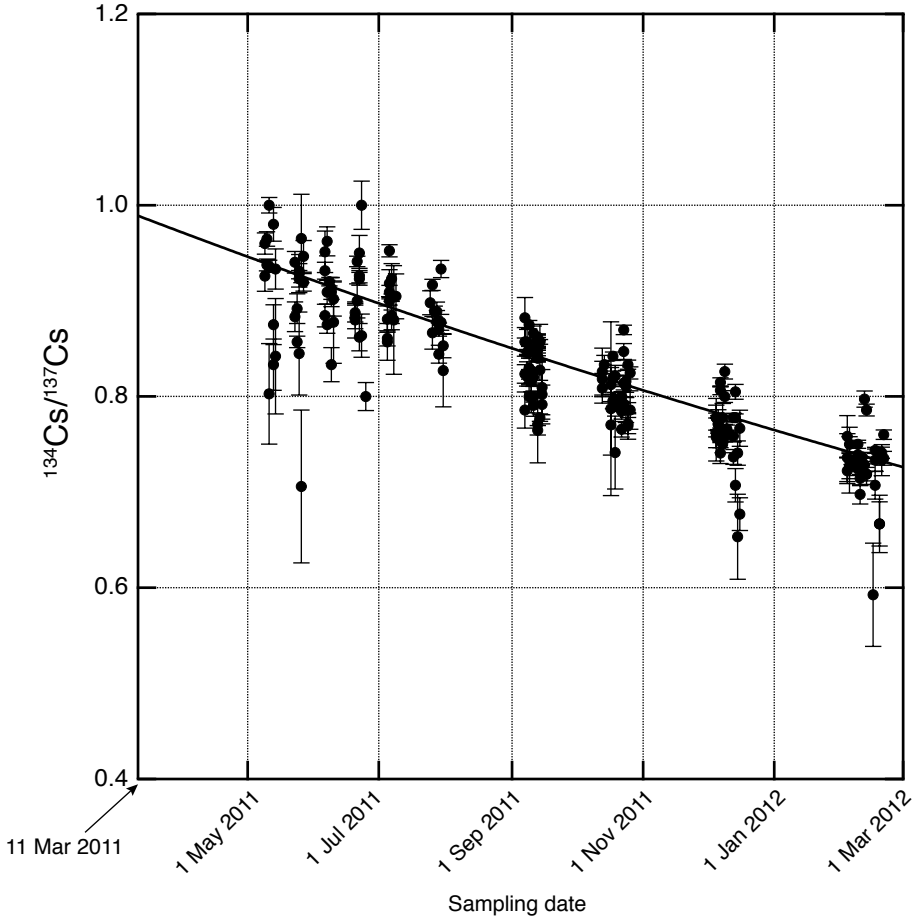

Fig. 6. Temporal variation of $^{134}Cs/^{137}Cs$ ratio in the sediments. The line represents the result of a weighted least-square fit and corresponds to the following equation: $^{134}Cs/^{137}Cs = c_1 \exp(-c_2 t)$, where $c_1 = 0.989$ and $c_2 = 0.000868$.

BGD
10, 4819–4850, 2013

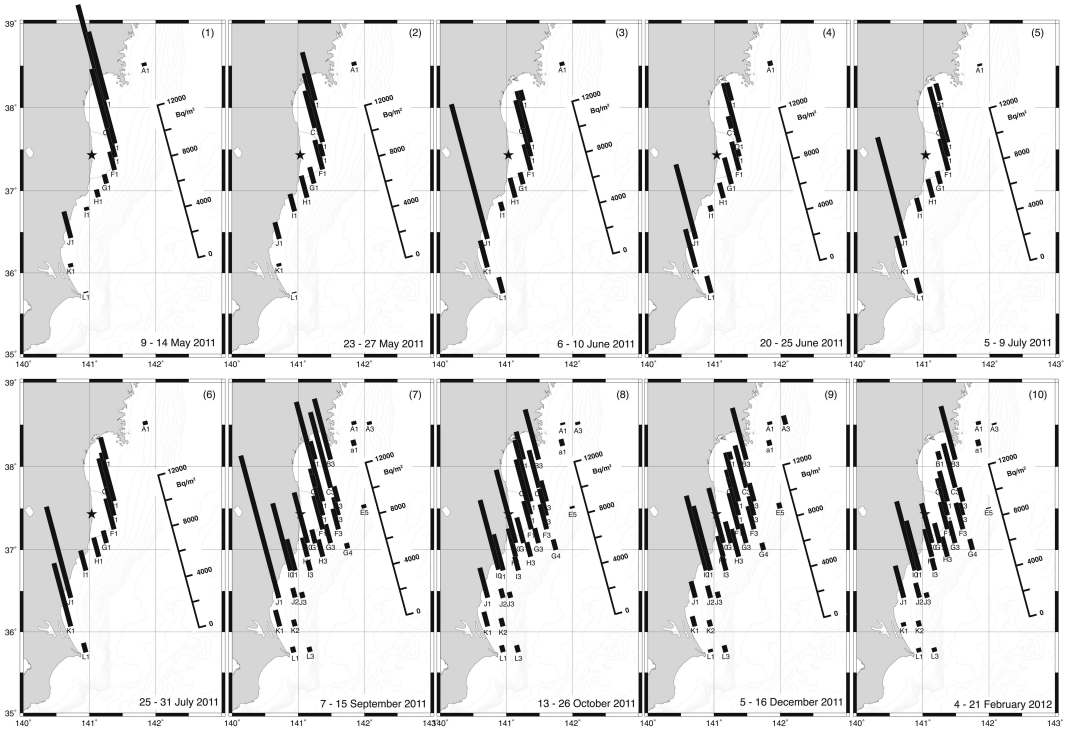

Fig. 7. Spatiotemporal variation of ^{137}Cs inventory in sediment samples collected on the dates indicated in the panels.

BGD
10, 4819–4850, 2013

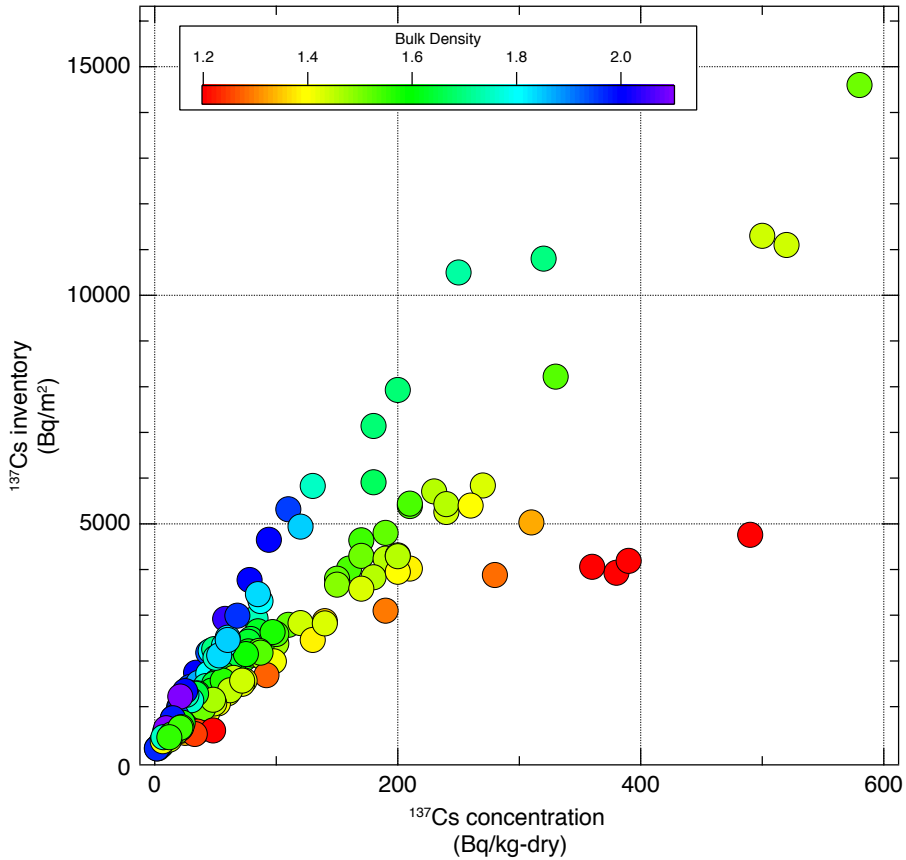

Fig. 8. Variation of ^{137}Cs inventory in sediment with ^{137}Cs concentration in sediment at various sediment bulk densities.

BGD
10, 4819–4850, 2013

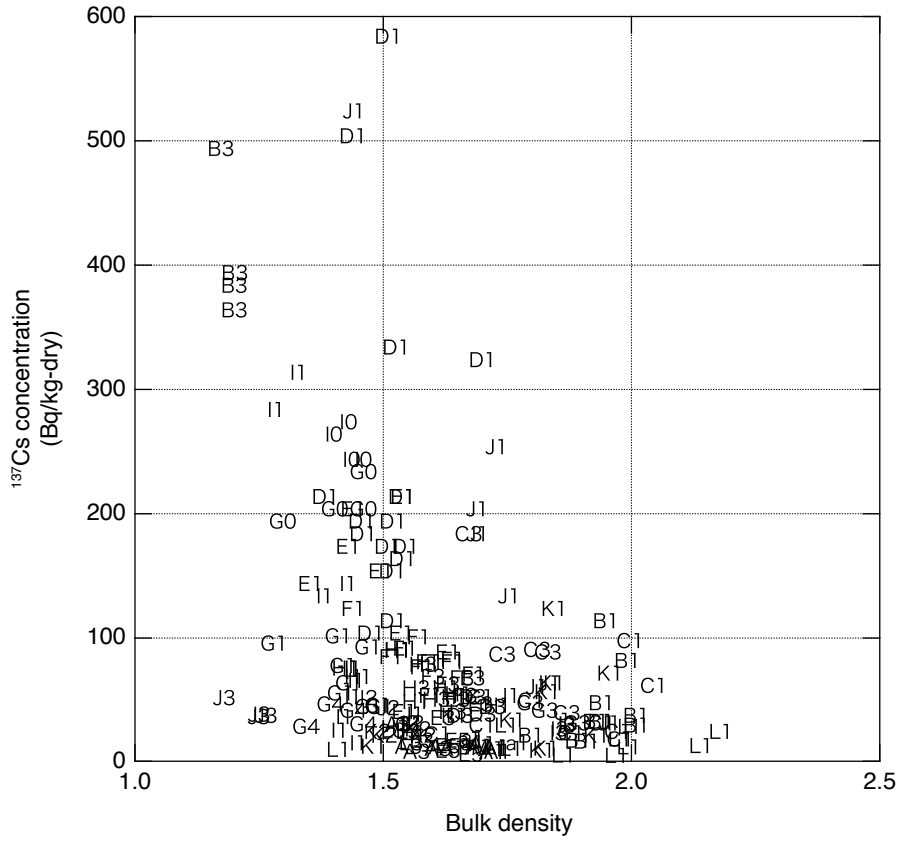

Fig. 9. Variation of ^{137}Cs concentrations with sediment bulk density at the sampling stations shown in Fig. 3.

BGD
10, 4819–4850, 2013

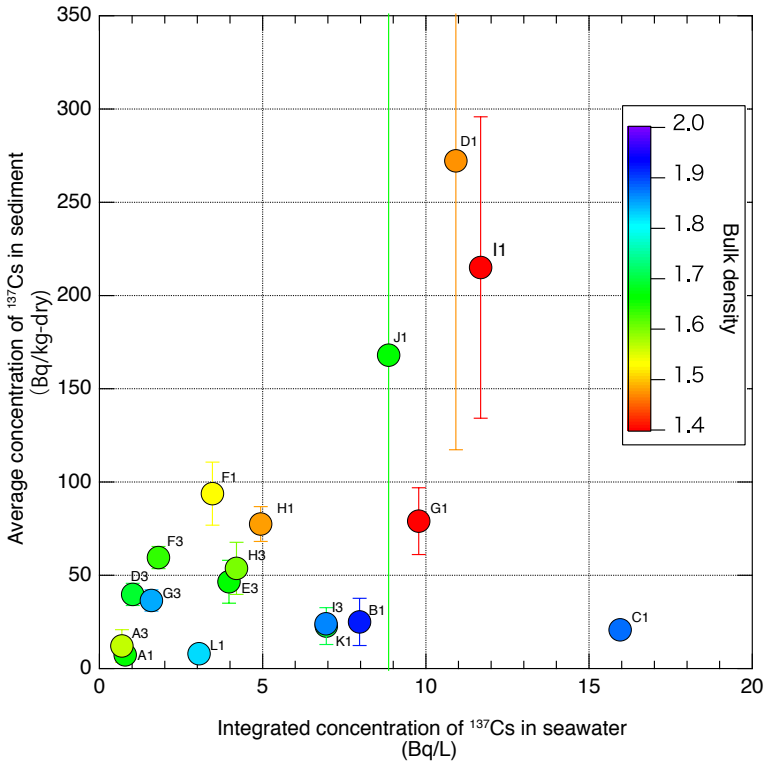

Fig. 10. Average ^{137}Cs concentrations in sediment, integrated ^{137}Cs concentrations in seawater, and average sediment bulk densities at each sampling station. Seawater concentrations obtained during six cruises from May to June 2011 were summed for each station. Average ^{137}Cs concentrations in sediment were calculated for samples obtained from September 2011 to February 2012. Error bars indicate the standard deviations of the sediment concentrations.

BGD
10, 4819–4850, 2013

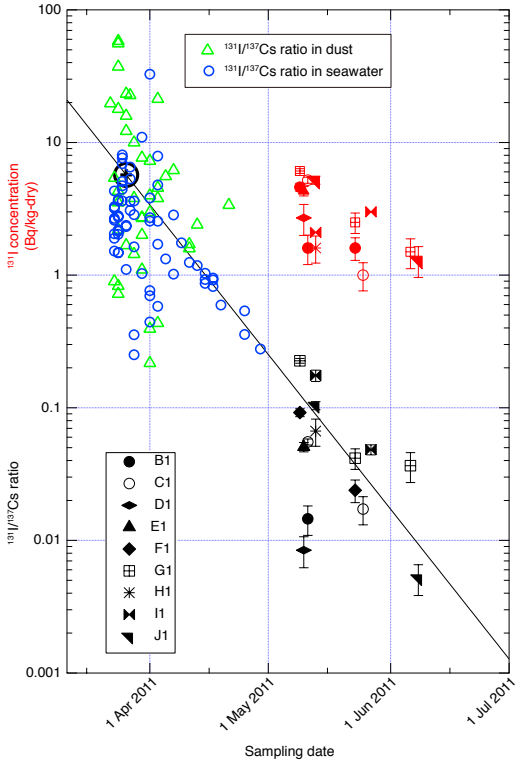

Fig. 11. Temporal variations of ^{131}I concentration and ^{131}I/^{137}Cs ratios in dust, seawater and sediment. The line shows the decay curve of the ^{131}I/^{137}Cs ratio based on an estimated initial ratio of 5.7 on 26 March 2011 (indicated by the circled cross; see Sect. 3.5 and Tsumune et al., 2012). ^{131}I/^{137}Cs ratios in dust and seawater were derived from data reported by MEXT (2012) and Oikawa et al. (2013), respectively.

BGD
10, 4819–4850, 2013

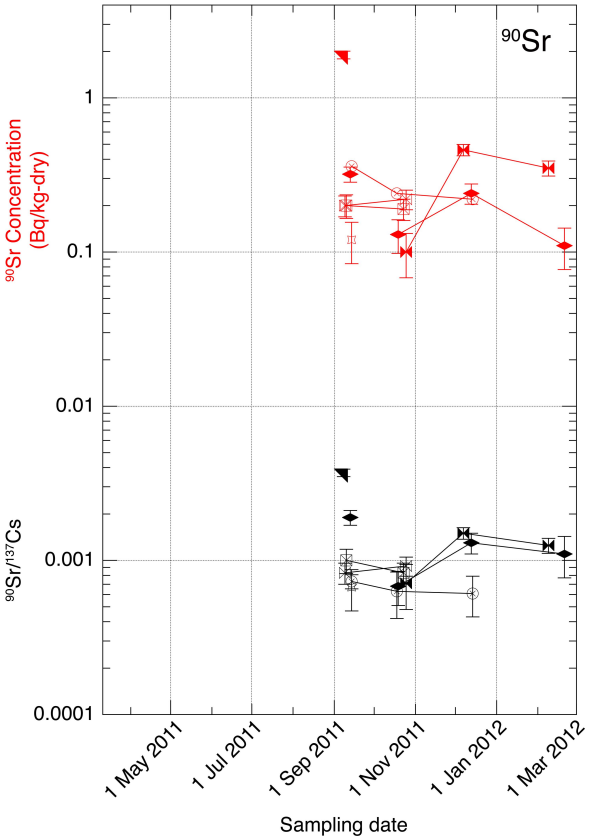

Fig. 12. Temporal variations of ^{90}Sr concentrations (red symbols) and ^{90}Sr/^{137}Cs ratios (black symbols) in the sediments. Values below the detection limit are not shown. See Fig. 13 for a key to the symbols.

BGD
10, 4819–4850, 2013

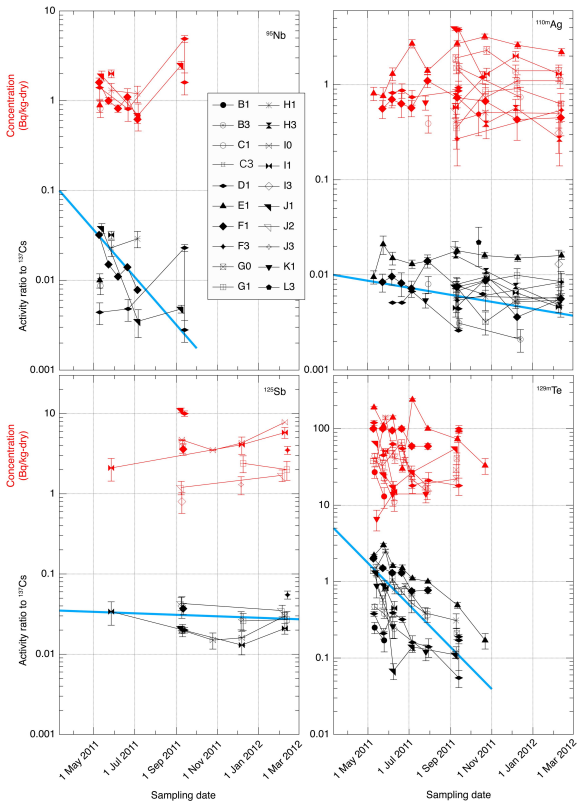

Fig. 13. Temporal variations of ^{95}Nb, ^{110m}Ag, ^{125}Sb, and ^{129m}Te concentrations (red symbols) and their corresponding ^{137}Cs activity ratios (black symbols) in sediments. The blue lines indicate theoretical decay curves for the nuclides at arbitrary initial values.

BGD
10, 4819–4850, 2013